Single-walled carbon nanotube bundles intercalated with semiconductor nanoparticles*

Manashi Nath[†,], Pallavi V. Teredesai[#], D. V. S. Muthu[#], A. K. Sood[†,#,‡] and C. N. R. Rao[†,**,‡]**

[†]Chemistry and Physics of Materials Unit, Jawaharlal Nehru Centre for Advanced Scientific Research, Jakkur P.O., Bangalore 560 064, India
[**]Solid State and Structural Chemistry Unit, Indian Institute of Science, Bangalore 560 012, India
[#]Department of Physics, Indian Institute of Science, Bangalore 560 012, India

Nanoparticles of CdSe, CdS and ZnSe have been incorporated in the inter-tubular gaps of single-walled carbon nanotube (SWNT) bundles. Electron microscope, X-ray diffraction (XRD), electronic spectroscopy and Raman studies have been employed to characterize these systems. The lengths of the intercalate inside the bundles could be varied by changing the reaction conditions. Electronic absorption and photoluminescence studies from the semiconductor intercalates show the expected blue-shift with respect to the corresponding bulk samples in CdS and ZnS samples. The SWNT lattice is expanded on incorporating CdSe as confirmed by XRD in the low-angle range. The expansion in the lattice is also corroborated by the Raman measurements which show a considerable red-shift for both the radial and the tangential modes of the SWNT signal, thus signifying an increase in the van der Waals gap between the tubes in the bundle. The red-shift of the Raman signal is due to the decrease in the inter-tube interactions as well as due to doping effects.

SINGLE-walled carbon nanotubes (SWNTs) are fascinating; they are not only of academic interest but also have potential applications[1], including nanoelectronics[2], pressure[3] and flow sensors[4] and actuators[5], high-strength composites[6], electron emitters[7] and hydrogen storage[8]. It has been shown that SWNTs assemble to form a triangular lattice, with an inter-tubular gap of ~ 3.2 Å. In this article, we show that the SWNT bundles can be used as templates to form nanocrystalline semiconducting systems in the van der Waals inter-tubular gaps. CdSe, CdS and ZnS quantum wires have been generated by this means.

The effect of quantum confinement in II–VI semiconductors on their physical, electronic and optical properties as a function of the aspect ratio, has been a subject of keen interest. Hu *et al.*[9] studied the polarized emission from colloidal CdSe quantum dots with aspect ratios varying from 1 to 30, and observed a sharp transition from non-polarized to purely linearly-polarized emission at an aspect ratio of 2. We have carried out photoluminescence studies

of the semiconductor intercalates and demonstrated the blue-shift of the band gaps due to quantum size confinement. Furthermore, we find that CdSe nanoparticles affect the inter-tubular spacings in the bundle with the inter-tubular gap increasing from 3.1 to ~ 3.6 Å with CdSe loading, as revealed by X-ray diffraction (XRD) measurements. Raman radial breathing mode and tangential modes of the SWNTs undergo red-shifts for CdSe loading, corroborating the expansion of the triangular lattice in the nanotube bundles. However, the red-shift of the modes cannot be accounted for fully only by the expansion of the lattice, suggesting that the intercalated CdSe results in electron doping of the nanotubes.

Experimental

The SWNTs were prepared by the procedure discussed elsewhere[1,10], purified by heating at ~ 320°C followed by treatment with 70% HNO₃. The purified SWNT bundles were refluxed in an aqueous solution of Cd or Zn salt (typically cadmium acetate or zinc acetate) overnight. The Zn and Cd-loaded SWNT bundles were subjected to sulphidation by warming in a solution of thioacetomide and NaOH, and further refluxed for a few hours. In order to obtain the selenide nanostructures, NaHSe solution was added drop-wise to a suspension of Cd-loaded SWNT bundles followed by refluxing for a few hours. The NaHSe solution was obtained by treating a suspension of Se in water with NaBH₄ in a He atmosphere. Different lengths of the CdSe/ZnS nano-intercalates inside the SWNT bundles were obtained by this method. The initial molar concentration of the salt solution affects the length of the nanostructure inside the SWNT bundles. These bundles were therefore refluxed in Cd/Zn-salt solutions of different molarities to obtain a range of lengths of the nano-intercalates.

Transmission electron microscope (TEM) images were acquired from a JEOL JEM3010 microscope operating at 300 kV. XRD patterns were recorded using CuK$_\alpha$ radiation with $\lambda = 1.5418$ Å. Photoluminescence (PL) from the intercalates was recorded at room temperature using a Perkin–Elmer fluorimeter. Raman measurements were

carried out at room temperature using DILOR XY triple-grating spectrometer equipped with liquid nitrogen-cooled charge coupled device, using 5145 Å line from an argon ion laser. These experiments were performed in the back-scattering geometry using confocal micro-Raman set-up with 100X objective (N.A. = 0.9), spot size of ~ 1.1 μm and power of ~ 1.2 mW.

Results and discussion

In Figure 1 *a–c*, we show typical TEM images to demonstrate the intercalation of the CdS nanoparticles in the inter-tubular space of SWNT bundles. The extent of intercalation could be varied by changing the concentration of the metal salt in the initial reaction mixture. Intercalation takes place in the inter-tubular space in the bundles and the thickness of the intercalates is generally around 0.34 nm, a value close to the van der Waals gap in the bundles. The length of the intercalate as seen in the sample with highest loading of CdS is ~ 90 nm. As the amount of CdS inside the bundle decreases, the length of the intercalate decreases, as can be seen from panels *b* and *c* in Figure 1.

The high-angle XRD patterns of the as-prepared semiconductor-intercalated SWNT bundles reveal the amorphous nature of the material inside the host. The CdS inside the SWNT bundles could, however, be crystallized

by heating the sample under argon atmosphere at 750°C. The high-angle XRD pattern of the heat-treated sample in Figure 2 *a* reveals the presence of peaks characteristic of hexagonal CdS, indicating that the semiconductor material has indeed been incorporated inside the SWNT bundles. Figure 2 *b* shows the absorption spectra of the CdS intercalates in the SWNTs. The longest intercalation of CdS inside the SWNT bundles shows a broad absorption peak
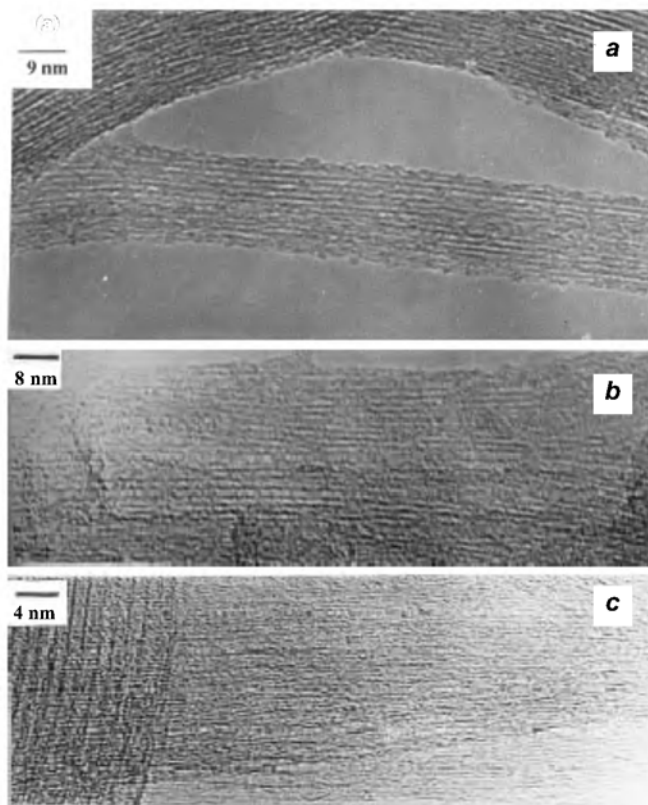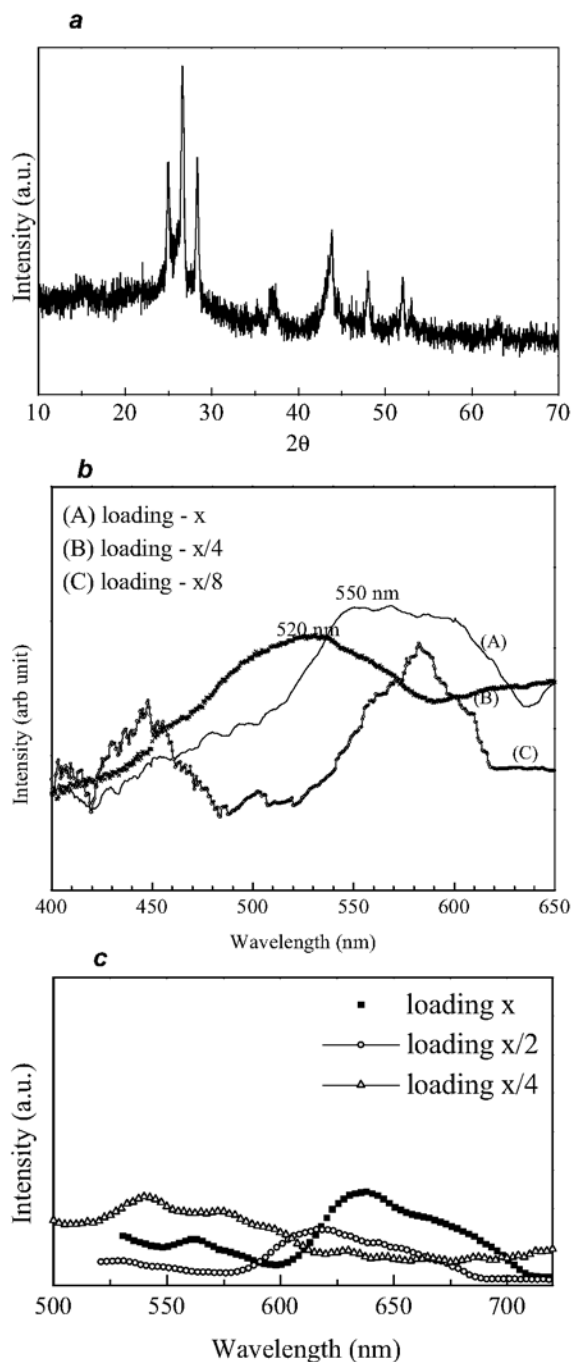
Figure 2. *a*, X-ray diffraction pattern of the heat-treated CdS-intercalated SWNT bundles; *b*, Absorption spectra of CdS-intercalated SWNT bundles with different loadings of CdS inside the bundles, and *c*, Photoluminescence spectra of SWNT bundles intercalated with CdS.

Figure 1. TEM images showing intercalated CdS in SWNT bundles. *a*, Highest loading; *b*, Intermediate loading, and *c*, Lowest loading.

at ~ 550 nm, which is blue-shifted as the length of the intercalate in the inter-tubular space inside the bundles decreases. The PL spectra of the corresponding samples are shown in Figure 2 c. The PL peak shifts to higher energies as the loading is reduced [bulk CdS shows a peak at 650 nm (attributed to the S vacancies and trap states)]. Thus, a quantum confinement is observed on decreasing the length of the CdS intercalate inside the SWNT bundles.

ZnS and CdSe nanostructures have also been incorporated in the inter-tubular spaces of the SWNT bundles. Figure 3 shows the TEM images for the ZnS and CdSe-intercalated SWNT bundles, respectively. The length of the intercalate was, however, much shorter in CdSe compared to CdS, the length being even shorter in the case of ZnS.

The ZnS intercalates inside the SWNT bundles also show characteristic electronic spectra. Figure 4 a and b shows the absorption and the PL spectra of ZnS-intercalated SWNT bundles, respectively. The absorption shoulder of bulk ZnS at ~ 330 nm is blue-shifted when ZnS is incorporated in the inter-tubular space. Bulk ZnS shows a PL band in the form of a doublet at 425 nm and 450 nm (solid line). The doublet becomes broader and shifts to higher energies as the loading is reduced, indicating quantum confinement.

Figure 5 shows room temperature XRD patterns of the pure SWNT bundles (I), SWNT bundles with the highest loading of CdSe (II) and ZnS (III). The low-angle diffractio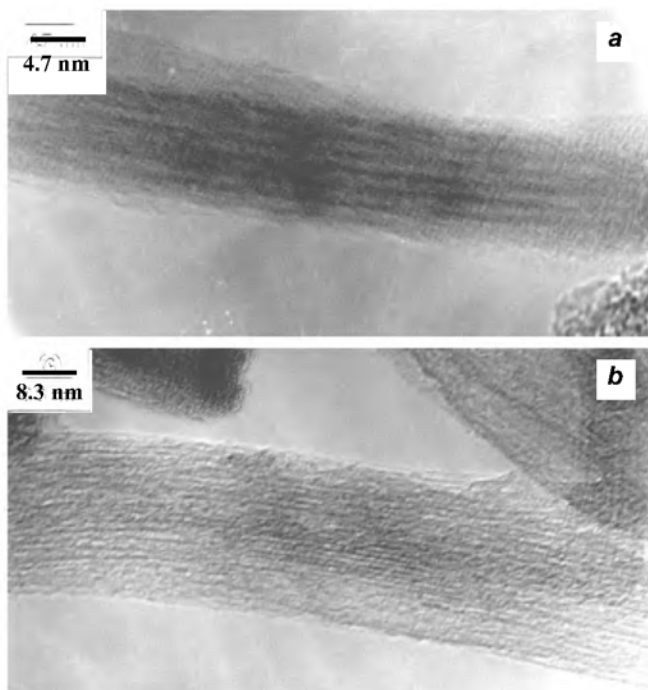n peak at $\theta \sim 3°$ in these XRD patterns corresponds to the Bragg reflection from the (100) planes of the two-dimensional triangular lattice of the nanotubes in a bundle. The low-angle XRD peak is obtained at 2.95° for pure (undoped) SWNT bundles. The low-angle peak shows a shift of 0.115°, as can be seen in Figure 5 (II) for highest loading of CdSe, corresponding to an increase in the d-value of 0.55 Å. The XRD pattern in low-angle region for the highest loading of ZnS, however, does not show any appreciable shift of the low-angle line, as seen in Figure 5 (III). The XRD pattern shows that there is considerable expansion of the 2D triangular lattice of the SWNT bundles when intercalated with CdSe.

The expansion of the SWNT lattice indicates an increase in the inter-tubular space and hence a decrease in the tube–tube interaction within the bundle. The radial mode (RBM) frequencies, ω_B, of the single-walled nanotubes are dependent on several factors, including the radius of the tube as well as the inter-tube separation,
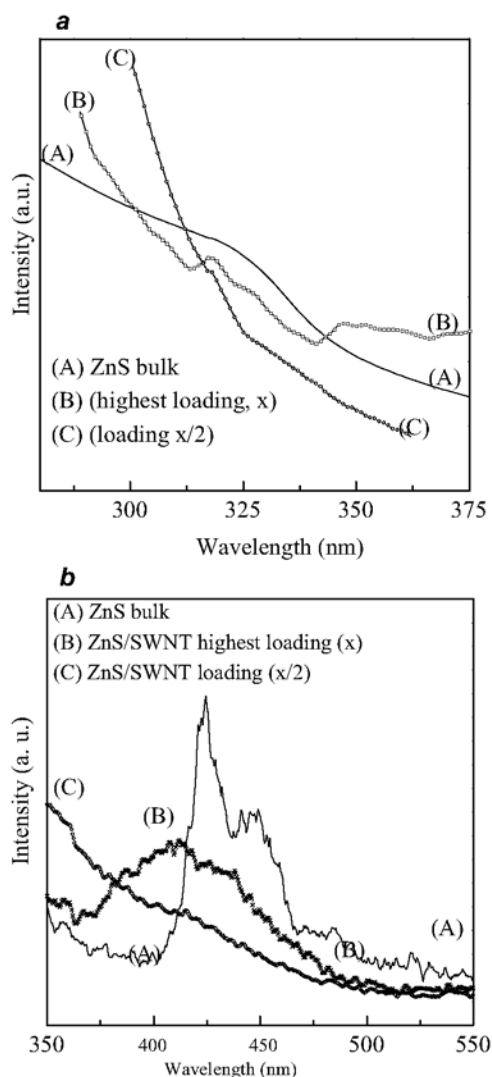

Figure 3. TEM images of the (*a*) CdSe and (*b*) ZnS intercalated SWNT bundles. The image in (*a*) clearly shows expansion of the spacing between the nanotubes.

Figure 4. (*a*) Absorption and (*b*) photoluminescence spectra of ZnS-intercalated SWNT bundles.

$$\omega_B = \Delta\omega + \frac{A}{d}, \qquad (1)$$

where ω_B is in units of cm^{-1} and diameter d in units of nm. The first term arises due to van der Waals interaction between the nanotubes in a bundle and is $\sim 14\ cm^{-1}$, i.e. ω_B of an isolated nanotube is red-shifted by $\sim 14\ cm^{-1}$ with respect to its value in the nanotube bundle. The parameter A, determined experimentally, is ~ 234 and is model-dependent. To investigate the effect of semiconductor intercalation on the vibrational properties of the SWNT bundles, we recorded the Raman spectra of the CdSe and ZnS-intercalated SWNT bundles. Figure 6 shows the Raman spectra for the radial and tangential (T) modes of the nanotubes for the highest loadings of CdSe-intercalated SWNT bundles (shown by black, solid lines) superimposed on the corresponding spectra of the pure SWNT bundles (shown by dotted lines). It is clear from Figure 6 that for CdSe intercalation, both the radial and tangential Raman modes are red-shifted relative to that of the pure SWNT bundles. The RBM frequency is red-shifted by $11\ cm^{-1}$, whereas the main T-mode is red-shifted by $4\ cm^{-1}$. For ZnS intercalation on the other hand, they remain almost unaffected.

There are two possible causes for the observed shifts in the Raman mode frequencies: (i) change in the van der Waals interaction between the tubes in a bundle (see first term in eq. (1)) and (ii) charge transfer between the nanoparticles and SWNT bundles. Based on theoretical calculations[11] the tube–tube interactions within a bundle result

in blue-shift of the RBM frequency maximum by $\sim 14\ cm^{-1}$ with respect to its value in the isolated tube[12]. From the low-angle XRD measurements, it was observed that the centre-to-centre distance between the nanotubes in the CdSe-intercalated bundles is larger compared to the undoped nanotube bundles. The diameter of the single-walled nanotubes in the bundle remaining unchanged after intercalation of CdSe, the expansion of the lattice leads to an increase in the inter-tubular space. Thus, as the inter-tubular space increases in the CdSe-loaded SWNT bundles, the inter-tube interaction decreases and the Raman mode is expected to show a red-shift of the radial modes. However, the observed shift of $\sim 11\ cm^{-1}$ of the RBM mode can only arise if the bundles completely breakdown on intercalation. But the TEM images of the intercalated tubes show that the tubes are still in the form of bundles, but with a larger inter-tubular separation. Further, such inter-tube interactions are not expected to affect the T-modes[12]. This leads us to suggest that part of the softening of RBM mode and the entire softening of the T-modes arise from doping effects. For graphite, it has been shown that introduction of electrons in the π^* band softens the intra-layer mode at $1579\ cm^{-1}$, while introduction of holes in the π band stiffens the intra-layer mode. Similarly, Rao et al.[13] showed that the T-modes in SWNTs are red-shifted on electron doping by $\sim 140\ cm^{-1}$ for one electron per carbon atom. Therefore, a red-shift of T-mode in CdSe-intercalated SWNTs will imply an electron doping of approximately one electron per 35 carbon atoms. Such charge transfer can occur between the semiconductor nanoparticles and the SWNTs, as the room temperature bandgap of CdSe (1.74 eV) is much higher than those between the van Hove singularities in pure semiconducting SWNTs (the lowest energy gap is $\sim 0.5\ eV$)[14]. However, further studies on the conductivities of the
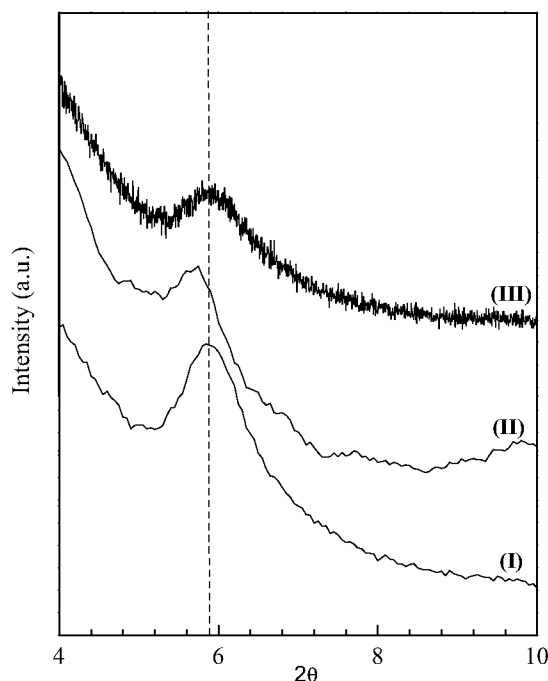

Figure 5. X-ray diffraction patterns for the low-angle peak of pure SWNTs (I) and those of SWNT bundles with highest loading of CdSe (II) and highest loading of ZnS (III).
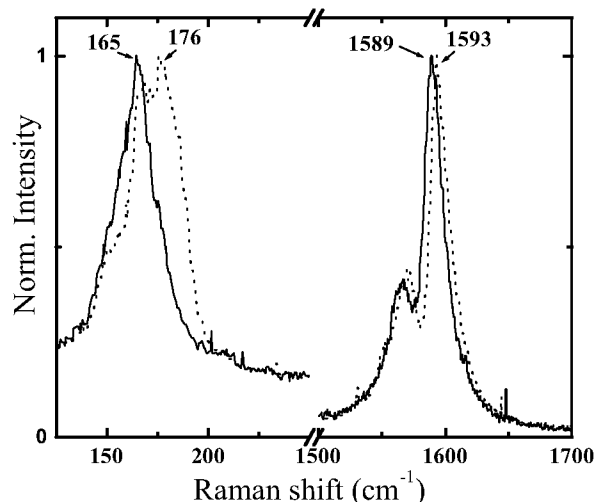

Figure 6. Raman spectra of the radial and tangential modes of SWNT bundles intercalated with CdSe (solid lines) along with the spectra of pure SWNT bundles (dotted lines).

CdSe-intercalated SWNT bundles are desirable to address this aspect of charge transfer in intercalated nanotubes.

In the case of ZnS-intercalated bundles, the inter-tubular space is not much expanded by the introduction of ZnS, possibly because of the lesser amount of ZnS intercalation, and hence the effect on the Raman modes is expected to be considerably smaller than in the case of CdSe intercalation, in agreement with our experiments.

Conclusion

Nanoparticles of semiconductors, CdS, CdSe and ZnS, could be incorporated in the inter-tubular space of the SWNT bundles. Absorption and PL bands from intercalated CdS and ZnS nanoparticles show blue-shifts as expected from quantum size effects. XRD measurements show that the inter-tube van der Waals gap in the nanotube bundles is enhanced by the intercalation of CdSe, whereas it remains almost unchanged in the case of ZnS. The shifts of the radial and tangential modes in the Raman spectrum of the SWNTs on intercalation can be explained, consistent with the XRD data, on the basis of changes in the van der Waals interactions between the tubes and the doping. It would be of interest to investigate the intercalation of other semiconductors and to theoretically address the question of charge transfer and structural stability of the intercalated nanotubes. Quantitative polarization studies of photoluminescence from the semiconductor intercalate as a function of the aspect ratio should also be carried out.

1. Rao, C. N. R., Satishkumar, B. C., Govindaraj, A. and Nath, M., Nanotubes. *Chem. Phys. Chem.*, 2001, **2**, 78–105.
2. Kruger, M., Buitelaar, M. R., Nussbaumer, T., Schonenberger, C. and Forro, L., Electrochemical carbon nanotube field-effect transistor. *Appl. Phys. Lett.*, 2001, **78**, 1291–1293.
3. Zhou, Q., Wood, J. R. and Wagner, H. D., Stress fields around defects and fibers in a polymer using carbon nanotubes as sensors. *Appl. Phys. Lett.*, 2001, **78**, 1748–1750.
4. Ghosh, S., Sood, A. K. and Kumar, N., Carbon nanotube flow sensors. *Science*, 2003, **299**, 1042–1044.
5. Baughman, R. H. *et al.*, Carbon nanotube actuators. *Science*, 1999, **284**, 1340–1344.
6. Dalton, A. B. *et al.*, Super-tough carbon-nanotube fibres. *Nature*, 2003, **423**, 703.
7. Sharma, R. B., Tondare, V. N., Joag, D. S., Govindaraj, A. and Rao, C. N. R., Field emission from carbon nanotubes grown on a tungsten tip. *Chem. Phys. Lett.*, 2001, **344**, 283–286; Fan, S., Chapline, M. G., Franklin, N. R., Tombler, T. W., Cassell, A. M. and Dai, H., Self-oriented regular arrays of carbon nanotubes and their field emission properties. *Science*, 1999, **283**, 512–514.
8. Gundiah, G., Govindaraj, A., Rajalakshmi, N., Dhathathreyan, K. S. and Rao, C. N. R., Hydrogen storage in carbon nanotubes and related materials. *J. Mater. Chem.*, 2003, **13**, 209–213.
9. Hu, J., Li, L. S., Yang, W., Manna, L., Wang, L. W. and Alivisatos, A. P., Linearly polarized emission from colloidal semiconductor quantum rods. *Science*, 2001, **292**, 2060–2063.
10. Teredesai, P. V., Sood, A. K., Muthu, D. V. S., Sen, R., Govindaraj, A. and Rao, C. N. R., Pressure-induced reversible transformation in single-wall carbon nanotube bundles studied by Raman spectroscopy. *Chem. Phys. Lett.*, 2000, **319**, 296–302.
11. Ghosh, S., Sood, A. K. and Rao, C. N. R., Electrochemical tuning of band structure of single-walled carbon nanotubes probed by *in situ* resonance Raman scattering. *J. Appl. Phys.*, 2002, **92**, 1165–1167; Sauvajol, J.-L., Anglaret, E., Rols, S. and Alvarez, L., Phonons in single wall carbon nanotube bundles. *Carbon*, 2002, **40**, 1697–1714.
12. Rao, A. M. *et al.*, Effect of van der Waals interactions on the Raman modes in single walled carbon nanotubes. *Phys. Rev. Lett.*, 2001, **86**, 3895–3898; Venkateswaran, U. D., Rao, A. M., Richter, E., Menon, E., Rinzler, A., Smalley, R. E. and Eklund, P. C., Probing the single-wall carbon nanotube bundle: Raman scattering under high pressure. *Phys. Rev. B*, 1999, **59**, 10928–10934.
13. Rao, A. M., Eklund, P. C., Bandow, S., Thess, A. and Smalley, R. E., Evidence for charge transfer in doped carbon nanotube bundles from Raman scattering. *Nature*, 1997, **388**, 257–259.
14. Wildoer, J. W. G., Venema, L. C., Rinzler, A. G., Smalley, R. E. and Dekker, C., Electronic structure of atomically resolved carbon nanotubes. *Nature*, 1998, **391**, 59–62.